

See discussions, stats, and author profiles for this publication at: <https://www.researchgate.net/publication/237045624>

O/Ag(100) Surface: A Density Functional Study with Slab Model

ARTICLE in THE JOURNAL OF PHYSICAL CHEMISTRY B · APRIL 2002

Impact Factor: 3.3 · DOI: 10.1021/jp012552p

CITATIONS

22

READS

30

4 AUTHORS, INCLUDING:



Yun Wang

Griffith University

89 PUBLICATIONS 1,154 CITATIONS

SEE PROFILE



Wenning Wang

Fudan University

74 PUBLICATIONS 1,185 CITATIONS

SEE PROFILE



Kangnian Fan

Fudan University

181 PUBLICATIONS 3,820 CITATIONS

SEE PROFILE

O/Ag(100) Surface: A Density Functional Study with Slab Model

Yun Wang, LingLing Jia, Wenning Wang, and Kangnian Fan*

Molecular Catalysis and Innovative Material Laboratory, Department of Chemistry, Fudan University, Shanghai 200433, People's Republic of China

Received: July 5, 2001; In Final Form: January 8, 2002

The structural and energetic properties of O/Ag(100) surface have been investigated using density functional theory (DFT) in conjunction with the plane wave basis sets. The periodic slab model is employed for the systems containing surface or subsurface O atoms at the normal or missing-row Ag(100) surfaces. Three surface cells: (1×1) , (2×2) and $(2\sqrt{2} \times \sqrt{2})$, are employed. The results show that the oxygen atoms at 4-fold hollow site for $p(1 \times 1)$ surface cell are slightly below the surface silver atoms. And the O atoms on the missing-row surface locate at the first silver layer. The hollow site is the most energetically preferred for O atomic adsorption on the (100) surface with different coverage. The adsorption energy at the hollow site on the $(2\sqrt{2} \times \sqrt{2})$ Ag(100) surface with the missing row structure at 0.5 ML is the highest in our studies. The surface and subsurface O atoms have different effects on the properties of substrate. The comparison of the O atomic adsorption on the three low-index Ag(111), Ag(100), Ag(110) surfaces is also reported.

Introduction

Transition metals play important roles in catalytic and electrochemical processes. The investigation of the interaction between atomic oxygen and metallic surfaces is rather crucial in these reactions. Silver has been paid more attention as a good catalyst^{1,2} and the electrode material.³ In the past 3 decades, the interactions between atomic oxygen and the silver surfaces have been studied by both experimental and theoretical chemists.^{4–16} But there are several fundamental questions about this system still unclear. According to the thermal desorption spectrum (TDS) results, Bao et al. classified the surface atomic oxygen on the electrolytic silver surface into three forms: the α species (surface atomic oxygen), the β species (bulk-dissolved oxygen), and the γ species (the subsurface oxygen).⁴ The former two species are regarded as the active centers to the oxidation, and the γ form is proposed as the dehydrogenation center.⁵ The theoretical studies of the O/Ag(110) surface by Sun et al. manifested the importance of subsurface O atom for the reactions such as methanol hydrogenation.^{6,7} The subsurface atomic oxygen was also suggested to play important roles on the epoxidation of ethene.⁸ But most former studies, experimental or theoretical, were focused on the surface atomic oxygen only. In addition, the former studies are focused on the (110) and (111) surfaces because they are prototypes of the loose and dense surfaces, respectively.^{5,6,9–12} The structural and electronic properties of subsurface oxygen atom at Ag(100) surface are still indistinct. However, the recent experiment¹³ implied that the subsurface O atoms under the first layer Ag atoms occur more easily on the Ag(100) surface than Ag(111) and Ag(110). The Ag(111) surface has dense atomic packing leading to high resistance for oxygen atom migrating from the surface to subsurface, and the Ag(110) reconstruction makes the subsurface oxygen atom unstable because of the known added O–Ag row.¹⁴ To understand the interaction between the atomic oxygen and the silver more completely, it is necessary to study the O/Ag(100) systems.

Some ultrahigh vacuum experiments were once performed on these systems. The high-resolution electron energy loss spectroscopy (HREELS) and low-energy electron diffraction (LEED) were employed in the study of O/Ag(100) by Fang.¹⁵ An ordered $c(2 \times 2)$ superstructure of the substrate at low temperature, and a $p(1 \times 1)$ structure above room temperature were suggested. Rocca et al. did some work to investigate the properties of the O/Ag(100) system recently.^{13,16–18} In their latest work, the phase transition of the atomic oxygen on Ag(100) was investigated by X-ray photoelectron spectroscopy (XPS), HREELS, X-ray photoelectron diffraction (XPD), and LEED. The probe reaction of CO oxidation was employed to study the chemical reactivity of different O species. At the low temperature, the missing-row $(2\sqrt{2} \times \sqrt{2})$ reconstruction of the substrate was proposed based on the HREELS and XPD results, and the oxygen atom was suggested to be on the 4-fold hollow site. The $p(1 \times 1)$ structure was found above 350K, the same as found by Fang. According to the binding energies of O1s electron from the XPS study by Rocca et al., three atomic oxygen species were detected on Ag(100) surface. The authors assigned the O530 (O1s binding energy was 530.3 eV) to the one slightly below the nearest surface Ag atoms at the missing row $(2\sqrt{2} \times \sqrt{2})$ reconstruction surface, which was inert to the CO oxidation. The O528 (O1s binding energy was 528.3 eV) was assigned to the surface one at the hollow site, which was the oxidation center of CO. And the O531 (O1s binding energy was 530.9 eV) was assigned to the subsurface oxygen. Although the simulation of XPD data by Rocca et al. illustrates some glancing pictures about the O/Ag(100) system, the experiments offer little direct structural and energetic information about this system. Furthermore, the superstructure of substrate after adsorption of atomic oxygen at the low temperature disaccords between the results by different experimenters. Theoretical computation is good at the investigation about the microcosmic structural and electronic properties, but there are little theoretical studies concerning the O/Ag(100) systems, especially those including subsurface oxygen. Ricart et al. once calculated O/Ag(100) surface with the cluster model,^{19,20} but only surface

* Corresponding author. Fax: +86-21-65641740. E-mail: knfan@fudan.edu.cn.

TABLE 1: Structure and the Work Function of Various Clean Silver Surface Cell

	(1 × 1) ^c	(1 × 1) ^d	(2 × 2)	(2√2 × √2)
<i>k</i> -points	17 × 17 × 1	12 × 12 × 1	6 × 6 × 1	4 × 8 × 1
<i>d</i> ₁₂ (Å)	2.05	2.05	2.05	2.04
<i>d</i> ₂₃ (Å)	2.10	2.09	2.09	2.09
<i>d</i> ₃₄ (Å)	2.09	2.10	2.10	2.10
<i>d</i> ₄₅ (Å)	2.09	2.08	2.09	2.09
φ ^b (eV)	4.33	4.33	4.33	4.34

^a *d*_{ij}: interlayer distance. ^b φ: work function value. ^c Eleven silver layers separated by nine layers of vacuum. ^d Six silver layers separated by six layers of vacuum.

atomic oxygen at the 4-fold hollow site above the surface was considered, and the substrate structure was fixed at the corresponding bulk data, which did not agree with the experiment. In the present study, we will investigate all the above-mentioned surface types using the slab supercell models to obtain the structural and energetic properties of O/Ag(100) surface. The results will strengthen our understanding about the interaction between atomic oxygen and the silver surface, and avail us to comprehend some complex oxidative mechanism on metallic surface.

Method

The density functional theory (DFT) methods are used in conjunction with the plane wave basis set. The computations are carried out with the program package VASP,^{21–23} which was developed at the Institut für Theoretische Physik of the Universität Wien. The electron–ion interaction is described by optimized ultrasoft Vanderbilt type pseudopotential,²⁴ supplied by G. Kresse and J. Hafner.²⁵ The plane wave cutoff energy is 300.0 eV. The general gradient approximation functional proposed by Perdew et al. known as PW91 is used.²⁶ The electronic ground state is calculated with the residuum-minimization techniques. The geometric structure is optimized with the conjugated-gradient technique. For the calculation of the fractional occupancies, a broadening approach proposed by Methfessel and Paxton²⁷ is used with a width of 0.2 eV. The repeated elongated slab supercell is used to model the (100) surfaces with six silver layers separated by six layers of vacuum. The positions of the O atom and Ag atoms in the upper four layers are allowed to relax, and the Ag atoms at the lower two layers are fixed at the ideal bulklike position (the theoretical lattice content *a*₀ = 4.17 Å), which was obtained from our former study.²⁸ The methods proposed by Makov²⁹ and Neugebauer³⁰ et al. are used to correct the error for the surface with a large dipole moment, where the energy converges slowly with respect to the *z* axle of the supercell. All the calculations of the O/Ag(100) systems are non-spin-polarized because the previous calculation on O/Ag(110) surface indicates that the interaction with silver surface results in a negligible spin moment on the oxygen atom.⁵ The Brillouin-zone integration has been performed using Monkhorst–Pack grids of special points.³¹ A (12 × 12 × 1) *k*-points mesh is used for the (1 × 1) surface cell, a (6 × 6 × 1) mesh for the (2 × 2) surface cell, and (4 × 8 × 1) for (2√2 × √2) surface cell. The clean surface structural and energetic properties of these surface cells are listed in Table 1. Compared with our former calculations with eleven silver layers separated by nine layers of vacuum,²⁸ the difference for the surface interlayer distance is about 0.01 Å, and the difference for the work function is 0.01 eV. It demonstrates that these supercell models and the corresponding *k*-points meshes are sufficient. The isolated O₂ dimer in the 10 × 10 × 10 Å³ cubic

TABLE 2: Structural and Energetic Properties of the O/Ag(100) (1 × 1) Surface Cell

	clean	H	B	OCT ^g	OCT ^h	TE
Δ ^a ₁₂ (%)	−1.8	31.1	−0.6	50.3	0.3	54.2
Δ ₂₃ (%)	0.5	−1.3	−0.5	0.9	50.8	−1.5
Δ ₃₄ (%)	0.5	1.2	−0.1	−0.5	−1.8	0.5
Δ ₄₅ (%)	0.0	0.2	−0.1	0.2	0.0	0.0
<i>d</i> ^b _{O–surf} (Å)		−0.33	1.37	−2.15	−3.08	−1.59
<i>d</i> ^c _{O–Ag} (Å)		2.11	2.01	2.15	2.15	2.17
Δ <i>E</i> ^d (eV)		3.47	2.42	2.89	3.06	2.98
φ ^e (eV)	4.33	4.43	8.01	4.48	4.37	4.68
Δφ ^f (eV)		0.10	3.68	0.15	0.04	0.35

^a Δ_{ij}: interlayer relaxation. ^b *d*_{O–surf}: distance from O atom to surface. ^c *d*_{O–Ag}: distance from O atom to the nearest Ag atom. ^d Δ*E*: energy change. ^e φ: work function value. ^f Δφ: the change of work function. ^g O atom at the first interlayer. ^h O atom at the second interlayer.

TABLE 3: Structural and Energetic Properties of the O/Ag(100) (2 × 2) Surface Cell

	clean	H	B	OCT	TE	<i>c</i> (2 × 2)–H	H–OCT
Δ ^a ₁₂ (%)	−1.8	0.2	−1.6	2.7	15.2	4.1	10.2
Δ ₂₃ (%)	0.3	0.3	0.1	13.8	0.2	−0.8	4.6
Δ ₃₄ (%)	0.6	0.7	0.1	0.8	0.7	0.2	0.2
Δ ₄₅ (%)	0.0	0.2	0.0	0.4	0.4	0.0	0.4
<i>d</i> ^b _{O–surf} (Å)		0.76	1.36	−2.59	−0.96	0.70	0.66 (−2.07)
<i>d</i> ^c _{O–Ag} (Å)		2.26	2.06	2.19	2.10	2.20	2.31 (2.30)
Δ <i>E</i> ^d (eV)		4.13	3.36	2.81	2.81	4.02	3.58
φ ^e (eV)	4.33	4.91	5.72	4.47	4.39	5.22	4.92
Δφ ^f (eV)		0.58	1.39	0.14	0.06	0.89	0.59

^a Δ_{ij}: interlayer relaxation. ^b *d*_{O–surf}: distance from O atom to surface. ^c *d*_{O–Ag}: distance from O atom to the nearest Ag atom. ^d Δ*E*: energy change. ^e φ: work function value. ^f Δφ: the change of work function.

TABLE 4: Structural and Energetic Properties of the O/Ag(100) (2√2 × √2) Surface Cell

	clean ^g	H ^g	2H ^g	clean ^h	H ^h	2H ^h
Δ ^a ₁₂ (%)	−2.0	1.2	4.8	−5.3	−0.4	7.2
Δ ₂₃ (%)	0.4	0.0	0.2	0.5	0.0	−0.9
Δ ₃₄ (%)	0.7	0.9	1.0	0.3	0.7	0.8
Δ ₄₅ (%)	0.1	0.4	0.5	0.2	0.3	0.1
<i>d</i> ^b _{O–surf} (Å)		0.69	0.70		0.31	0.17
<i>d</i> ^c _{O–Ag} (Å)		2.19	2.20		2.10	2.11
Δ <i>E</i> ^d (eV)		3.99	3.94		4.15	4.21
φ ^e (eV)	4.34	4.72	5.27	4.32	4.56	4.70
Δφ ^f (eV)		0.39	0.93		0.24	0.38

^a Δ_{ij}: interlayer relaxation. ^b *d*_{O–surf}: distance from O atom to surface. ^c *d*_{O–Ag}: distance from O atom to the nearest Ag atom. ^d Δ*E*: energy change. ^e φ: work function value. ^f Δφ: the change of work function. ^g For the normal surface. ^h For the missing-row reconstruction surface.

supercell is calculated to verify the validity of the oxygen soft pseudopotential with the same energy cutoff 300.0 eV. The spin polarization is considered. The calculated bond length is 1.24 Å, and the binding energy is 6.60 eV. These data are the same as the recent work of Liem et al.³²

Results

In Tables 2–5, the relaxation of the uppermost layers (Δ₁₂, Δ₂₃, Δ₃₄, and Δ₄₅) is given as a percentage of the ideal interlayer distance. Both the distances from oxygen atom to the mass center of the surface (*d*_{O–surf}) and to the nearest silver atom (*d*_{O–Ag}) are given in the tables. The minus sign of the *d*_{O–surf} means that the oxygen atom is below the uppermost Ag layer. The energy change (Δ*E*) is defined by the formula of Δ*E* = −(*E*_{O–substrate} − *E*_{substrate} − *N**E*_O)/*N*, where *E*_{substrate} and *E*_{O–substrate} are the total energies of the systems with or without O atoms, respectively, and *E*_O presents the energy of the isolated oxygen atom calculated with spin polarization. *N* is the number of the

TABLE 5: Structural and Energetic Properties of O on the Different Single Crystal Surfaces

	Ag(110)	O–Ag(110)	Ag(100)	O–Ag(100)	Ag(111)	O–Ag(111)
Δ_{12}^a (%)	−9.6	−4.9	−1.8	0.2	−0.3	−1.4
Δ_{23}^a (%)	2.2	1.4	0.3	0.3	−0.2	−0.3
Δ_{34}^a (%)	−1.9	4.4	0.6	0.7	0.1	−0.5
Δ_{45}^a (%)	1.2	−2.4	0.0	0.2	−0.1	−0.7
$d_{\text{O-surf}}^b$ (Å)		0.49		0.76		1.22
$d_{\text{O-Ag}}^c$ (Å)		2.41		2.26		2.15
ΔE^d (eV)		3.88		4.13		3.74

^a Δ_{ij} : interlayer relaxation. ^b $d_{\text{O-surf}}$: distance from O atom to surface. ^c $d_{\text{O-Ag}}$: distance from O atom to the nearest Ag atom. ^d ΔE : energy change.

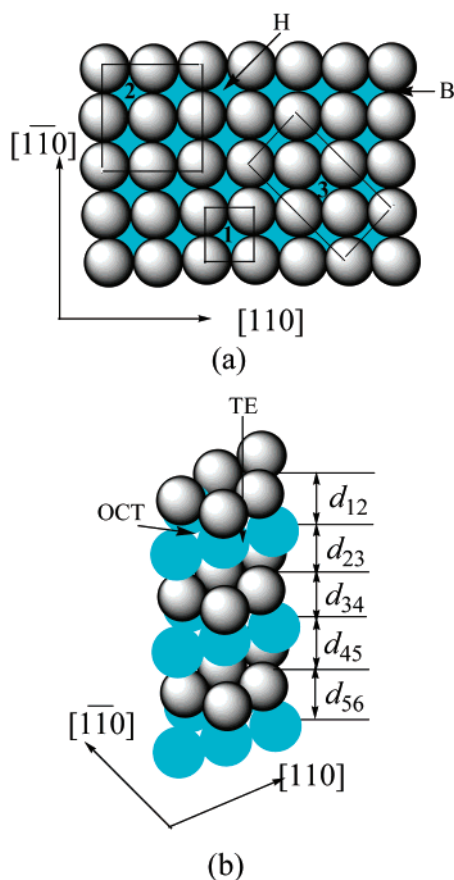


Figure 1. Schematic representation of the Ag(100) surface. (a): top view of the surface. The numbers 1–3 represent different surface cell: 1. (1×1) ; 2. (2×2) ; and 3. $(2\sqrt{2} \times \sqrt{2})$. (b) Side view of the surface. The silver atoms in the adjacent layers are expressed with the different balls.

O atoms in the surface cell. The change of work function value is calculated with the formula $\Delta\phi = \phi_{\text{O-surface}} - \phi_{\text{surface}}$, where the ϕ_{surface} is the work function value of the clean silver surface, and $\phi_{\text{O-surface}}$ is the work function value of the system with O atom. The work function value ϕ is defined by the formula $\phi = E_{\text{vac}} - E_{\text{F}}$, where E_{vac} is the vacuum energy, and E_{F} is the Fermi energy of the system. The vacuum energy is estimated by averaging the electrostatic potential of the vacuum layers.

1. (1×1) Surface Cell. Both Rocca et al. and Fang reported that the stable (1×1) phase was observed above the room temperature.^{13,15} In our present studies, several high-symmetry sites: the bridge site (B), the 4-fold hollow site (H), the octahedral interstitial site (OCT), and the tetrahedral interstitial site (TE) are selected as the position of the atomic oxygen (Figure 1). The top site is not considered, because the O atom at the top site has only one nearest Ag atom, and the top site would not be an energetically preferred one. The theoretical

results of O/Ag(100) (1×1) surface cell are listed in Table 2. Because the O atom at OCT site does not stay in the second layer perfectly, two situations are observed. One is that the O atom stays between the first and the second layer, and the other is that the O atom locates at the second interlayer. In our studies, the H site is the most energetically favorite one, where O atom sits slightly below the uppermost Ag atoms. The adsorption energy ΔE at the surface B site is the smallest.

In Table 2, the relaxation of all interlayer distances reduces when the surface O atom at B site. At other sites, the subsurface O atom enlarges the interlayer distance where it sits, but it changes the other interlayer distances slightly. This implies that the O atom has little interaction with the layers except the nearest ones. The surface O atom at the B site enhances the system work function greatly ($\Delta\phi = 3.68$ eV), while the subsurface O atom has little effect on the system work function (Table 2). The large value of the work function change for the bridge adsorption is due to the great enhancement of the vacuum energy of the system. The high concentration of the surface oxygen atom at B site prevents the escape of the surface electrons to the vacuum. The values of $\Delta\phi$ for subsurface O/Ag(100) systems are less than 0.4 eV. The small value of $\Delta\phi$ at H site may be due to subsurface position of the oxygen, which has negative dipole. The values of $\Delta\phi$ at other subsurface sites relate to the distances from oxygen to surface. The large distance will reduce $\Delta\phi$. The rather small value of $\Delta\phi$ at the OCT site between the second and the third layer indicates that the O atom has little effect to the charge densities of surface Ag atoms.

2. (2×2) Surface Cell. The theoretical results of the (2×2) surface cell are listed in Table 3. The same as the (1×1) surface cell, we have investigated the bridge site (B), 4-fold hollow site (H), octahedral interstitial site (OCT), and tetrahedral interstitial site (TE) (Figure 1). The most energetically favorite site is still the H site. The adsorption properties under the low coverage ($\Theta = 1/4$ ML) is much different from those in the (1×1) surface cell. The O atom prefers staying above the surface to site below the surface. The O atom at OCT site is stable only at the second interlayer. The values of ΔE at subsurface TE and OCT sites are smaller than that at surface H and B sites. In addition, the corresponding values of ΔE at subsurface sites in this case are smaller than those under the coverage $\Theta = 1$ ML. The effect of the coverage will be discussed in the following section.

The structure of substrate becomes corrugated after adsorption or penetration of O atom. Same as the (1×1) surface cell, the relaxation of substrates is slight when oxygen atom sits above the surface. The distance of the two adjacent layers, which accommodates the O atom, increases significantly. Because we calculate the substrate relaxation using the distance between the mass centers of the layers, the values of relaxation under the coverage $\Theta = 1/4$ ML are smaller than that in the (1×1) surface cell. The work function increases obviously when O atom sits above the surface, while it increases only slightly for the

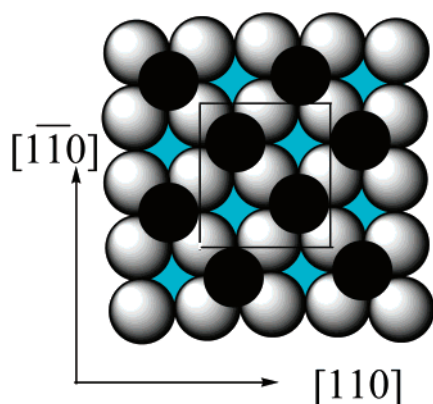


Figure 2. The illustration of the $c(2 \times 2)$ O/Ag(100) surface. The black balls present the oxygen atoms. The others are silver atoms.

existence of the subsurface O atom. The increase of the work function value at TE site is 0.06 eV, which is almost negligible.

The $c(2 \times 2)$ surface is also investigated by putting two O atom at the H sites along the $\langle 1\bar{1}0 \rangle$ orientation with the $\frac{1}{2}$ coverage (Figure 2). Fang once proposed this structure from the HREELS and LEED experiments.¹⁵ The results are listed in Table 3. Comparing the results of $c(2 \times 2)$ surface with that of the H site with the coverage $\Theta = \frac{1}{4}$ ML, we find that the O atom is closer to surface and the nearest silver atoms, but ΔE decreased slightly. The work function increases along with the increase of coverage. From Table 3, we also find that the high coverage of O atom changes the first and the second interlayer distances considerably. Compared with the ideal interlayer distance, the first interlayer expands, and the second one contracts. These are contrary to the clean Ag(100) surface relaxation, and these are also much different from those with low coverage $\Theta = \frac{1}{4}$ ML.

In fact, the surface and the subsurface O atoms are coexistent, which has been demonstrated by XPS.¹³ There have been no theoretical studies to investigate such systems. The model including one O atom at H site and another one at OCT site is scrutinized in this study. The energetic and structural results are listed in Table 3. The data in the parentheses are those with O atom at OCT interstitial. The effect of the surface O atom on the subsurface O atom is observed. Without the surface O atom, the O atom at OCT interstitial prefers staying between the second and the third layers under the coverage $\Theta = \frac{1}{4}$ ML. With an additional O atom at H site, the OCT oxygen atom is in the first interlayer. The substrate structure becomes more corrugated with the coexistence of the two kinds of O atoms. The $d_{\text{O-surf}}$ and $d_{\text{O-Ag}}$ are both different from those with single O atom. The O atom at H site with subsurface O atom is closer to the surface, while it is farther from the nearest Ag atoms. The larger $d_{\text{O-Ag}}$ is caused by the surface corrugation. Although noticeable differences are found for the first and the second interlayer relaxation, the third and fourth interlayer distances change slightly, similar to the cases of the clean silver surface and the other O/Ag(100) systems. The average ΔE is smaller than that with one O atom at the H site, and larger than that with one O atom at OCT site. The work function value of the two-O-atom system is close to that of H-site adsorption. It again demonstrates that surface O atom determines the change of work function, and subsurface O atom has little effect on the surface electronic properties. The two-O-atom system with the O atoms at H site and TE site are also investigated, but it is unstable. The O atom cannot stay at TE site with the existence of the surface O atom.

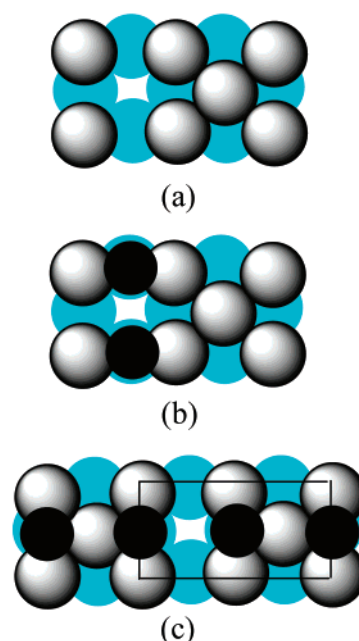


Figure 3. The illustration of the missing-row $(2\sqrt{2} \times \sqrt{2})$ Ag(100) surface cell. (a) clean surface; (b) one oxygen atom at the H site; (c) two oxygen atoms at the H sites.

3. $(2\sqrt{2} \times \sqrt{2})$ Surface Cell. This surface cell model is investigated because Rocca et al. proposed one missing-row reconstruction of substrate after an O atom adsorption at low temperature.¹³ There have been again no theoretical studies of the O/Ag(100) systems with defect before. At first we investigate the clean $(2\sqrt{2} \times \sqrt{2})$ surface (Figure 1), and then the systems with one O atom at H site and two O atoms at H site along the $\langle 100 \rangle$ orientation, which is suggested by Rocca et al.. The results are listed in Table 4. The properties of the system with one O atom at H site in $(2\sqrt{2} \times \sqrt{2})$ surface cell are different from those in (2×2) surface cell, since they have different symmetry. The first interlayer distance expands considerably, and the O atom is closer to the substrate surface and the nearest silver atoms in the $(2\sqrt{2} \times \sqrt{2})$ surface than in the (2×2) surface, while ΔE and $\Delta\phi$ are lower. The energetic and structural properties with two O atoms on both $(2\sqrt{2} \times \sqrt{2})$ surface and (2×2) surface are similar. It indicates the similar interaction between O atoms and the Ag atoms for these two systems under same coverage.

We have also investigated the missing-row reconstruction Ag $(2\sqrt{2} \times \sqrt{2})$ surfaces with and without adatoms (Figure 3). The theoretical results are listed in Table 4. The structure of the clean missing-row Ag(100) surface is much different from the normal one. The first interlayer distance contracts 5.3%, compared with the ideal interlayer distance. The Δ_{12} of normal surfaces are less than 2%, but the other interlayer distances of the reconstruction surface are close to those of the normal surfaces. The low coordination of the surface Ag atoms leads to stronger interaction between the surface atoms and the second layer atoms. The surface Ag atoms move laterally, and are closer to its nearest Ag atoms. Furthermore, the work function value decreases slightly since the surface atom density reduces.

The O atoms at H site on the Ag $(2\sqrt{2} \times \sqrt{2})$ missing-row surface are almost within the same layer of the uppermost Ag atoms, and $d_{\text{O-Ag}}$ shortens considerably. The value of ΔE is larger than that in the normal surfaces because of more highly unsaturated coordination of the surface Ag atoms. Our optimized results with two O atoms at H sites (Figure 3c) are different

from the model proposed by Rocca et al. in their simulation of XPD data.¹³ They suggested that the two O atoms be almost in the same layer of the uppermost Ag atoms, and one line of Ag atoms are slightly higher than the O atoms. They used this model to explain the decreased work function reported by Engelhardt and Menzel about 2 decades ago.³³ In our studies, no Ag atom is higher than the O atoms, and the O atoms are 0.17 Å above the surface Ag atoms. The values of $\Delta\phi$ are small, but still positive.

4. Surface Oxygen on Different Silver Single-Crystal Surfaces. We have demonstrated that the properties of the different single crystal surface depend significantly on the surface atom packing.²⁸ To compare the properties of O adsorption on different silver single-crystal surfaces systematically, the calculations of O/Ag(110) and O/Ag(111) systems are performed. There were some previous theoretical studies about the interactions between O atom and the (110), (111) surfaces. Gravil et al. and Sun et al. calculated the O/Ag(110) with the slab model.^{6,9} Salazar et al. investigated the O/Ag(111) with the cluster model recently.¹¹ We calculated these systems using the slab model. The (2×2) (110) surface cell with $(6 \times 6 \times 1)$ k -points mesh and $(\sqrt{3} \times \sqrt{3})$ Ag(111) surface cell with $(8 \times 8 \times 1)$ are selected here. All the supercells contain six layer substrates separated by vacuum with same depth. The upper four silver layers are allowed to relax and the lower two layers are fixed at the ideal position. The O atom is adsorbed at the 4-fold hollow site of Ag(110) surface, and at the 3-fold fcc hollow site of Ag(111) surface. Although some previous studies reported that long-bridge site is preferred for the O atom adsorption on the (110) surface, Gravil et al. demonstrated that hollow site is more energetically favorite under the low coverage.⁹ Our theoretical results are listed in Table 5.

Discussion

From Tables 2–4, we find that the properties of the O/Ag(100) is related to the coverage. The O atom is above the surface under the low coverage, and below the top Ag atoms with the coverage $\Theta = 1$ ML. So the $p(1 \times 1)$ structure could not be observed under the room-temperature by experiments. The distance of the interlayer which accommodates the O atom expands about 50% with the coverage $\Theta = 1$ ML. The relaxation of such interlayer with the low coverage expands less than 16%. The O atom at OCT site can stay between the first and the second interlayer with high coverage, but only stays at second interlayer with low coverage. Compared with the work function at the surface B site, the $\Delta\phi$ increases significantly with the coverage enhancement. The effect of the surface O atom to the substrate structure is also related to the coverage. But from Tables 2 and 3, we find that the effect of the subsurface O atom on the work function is independent of the coverage.

The surface O atom has different effect on the substrate structural and electronic properties from that of the subsurface O atom. The subsurface O atom enlarges the interlayer distance significantly, while the surface O atom has the substrate structure only change slightly. The values of $\Delta\phi$ with the surface O atom adsorption are higher than those with the subsurface O atom. The interaction between the surface and the subsurface O atoms is considerable. The surface O atom stabilizes the subsurface O atom at the OCT site, and the subsurface O atom makes the surface one at H site to move to substrate. So the surface catalytic reaction mechanism must be complicated. The surface adatoms mainly change the substrate electronic properties. The nearest silver atoms turn into Lewis acid centers. It benefits the adsorption of some reactant.³⁴ The subsurface O atoms

change the structural properties of substrate considerably. Some subsurface O atoms are close to the uppermost silver atoms, so they are the Lewis base sites. They might interact with the hydrogen atom of some reactants, and become the dehydrogenation center.

The O atoms far below the top silver atoms such as those at the OCT site in the second interlayer with the coverage $\Theta = 1$ ML, and O atoms very close to the surface such as those at the H site with the coverage $\Theta = 1$ ML or at TE site with the coverage $\Theta = 1/4$ ML, enhance the system work function only slightly. The former case indicates that the effect of the O atom is limited on the electronic properties of the Ag atoms, which are far from oxygen. The later case is caused by the negative charge of the O atom, which is so close to the interface. Both $d_{\text{O-surf}}$ in these systems are less than 1 Å. Because of such a short $d_{\text{O-surf}}$ and the negative charge on O atom, it is easy to understand the important effect of the subsurface oxygen on some catalytic reactions.^{5,8} The decrease of the work function reported by experiment³³ is not observed in our study. We suggest that the decrease of the work function be caused by more complicated situation, such as the other surface defect.

The values of the ΔE are larger when oxygen is adsorbed at the missing-row surface. This indicates that, if this surface defect exists, the O atoms will be adsorbed on the defective sites. Compared with the surface relaxation for the O atom adsorption at the normal surface, the influence of the O atom to the structure of the missing-row surface is stronger. The change of the first interlayer distance is from -5.3% for the adsorption of one O atom to $+7.2\%$ for the adsorption of two O atoms at H sites.

From Table 5, we find that the adsorption of O atom at H site reduces the substrate relaxation apparently on (110) or (100) surface, and changes the (111) surface structure slightly. It is related to the atomic packing of the surface. The relaxation of Ag atoms at the third and forth layer is still large for the O/Ag(110) surface. This is due to short interlayer distance of Ag(110) surface, which is only $0.354a_0$ (a_0 is the lattice constant). Because of the strong relaxation of the O/Ag(110) surface, the reconstruction, such as added-row structure, was reported by experiment.¹⁴ There is slight relaxation on O/Ag(111) surface, and no reconstruction was reported for this system. The relaxation of O/Ag(100) surface at H site is not significant with the low coverage, while it becomes noticeable with the increase of the coverage. But the distances of the second and lower interlayer are almost the same as the ideal one. It implies that the formation of the missing-row reconstruction of Ag(100) surface induced by the adsorption of oxygen atoms is hard to occur even with the high coverage of oxygen. The $d_{\text{O-surf}}$ for (110) surface is the shortest, but the $d_{\text{O-Ag}}$ is the longest. This is due to that the Ag(110) surface has more open structure. So for (111) surface with dense atomic packing, the values of $d_{\text{O-surf}}$ and $d_{\text{O-Ag}}$ show the contrary trend. From Table 5, it is found that the value of ΔE for (100) surface is higher than that for (110) or (111) surfaces. This is also observed when we studied the iodine modified silver surfaces.³⁵ This owes to the short $d_{\text{O-Ag}}$ and the four coordination of O atom on the (100) surface.

Conclusion

The interaction between the O atom and the Ag(100) surface are studied. Both the normal surface and the missing-row substrate are considered, and both the surface and the subsurface O atom are investigated in our studies. The O atom has strong interaction only with the nearest Ag atoms. The 4-fold hollow site is the most energetically favorite one among our considered sites. The properties of O/Ag(100) surface are related to the

coverage. The adsorption energy at the hollow site on $(2\sqrt{2} \times \sqrt{2})\text{Ag}(100)$ surface with the missing row structure at 0.5 ML is the highest. This matches with the experience. The surface O atom makes the work function change considerably, while the subsurface O atom impacts the substrate structure significantly. The different properties between systems comprising the surface or subsurface atomic oxygen give an explanation about the different catalytic function about the surface and subsurface oxygen. The adsorption of the surface oxygen atom lead the nearest silver atoms turn into Lewis acid site. It benefits the adsorption of the other adsorbate. The subsurface oxygen atom at TE site is close to the surface, which can be proposed as the Lewis base site. It is good to the dehydrogenation of the reactants. When the surface and the subsurface O atoms coexist, both the surface structure and work function change greatly. The influence of surface O atom to the subsurface one is significant.

The distance of the first interlayer for the missing-row surface contracts more greatly than that for the normal surface. The O atoms at the reconstruction surface stay almost at the same layer of the uppermost silver atoms. The O atom at the missing-row surface makes the system work function change only slightly. The interactions between surface oxygen atoms and different single-crystal surfaces are discussed, and they depend on the surface atomic packing.

Acknowledgment. We are grateful to the Shanghai Supercomputer Center for the computer time of the Shenwei supercomputer. This work was supported by the National Natural Science Foundation of China (Grant 29892167).

References and Notes

- (1) Jones, R. G. *Prog. Surf. Sci.* **1988**, 27, 25.
- (2) Campbell, C. T.; Paffett, M. T. *Appl. Surf. Sci.* **1984**, 19, 28.
- (3) Hubbard, A. T. *Chem. Rev.* **1988**, 88, 633.
- (4) Bao, X.; Lehmpfuhl, G.; Weinberg, G.; Schlögl, R.; Ertl, G. *J. Chem. Soc., Faraday Trans.* **1992**, 88, 865.
- (5) Schubert, H.; Tegtmeier, U.; Herein, D.; Bao, X.; Muhler, M.; Schlögl, R. *Catal. Lett.* **1995**, 33, 305.
- (6) Sun, Q.; Wang, Y.; Fan, K. N.; Deng, J. F. *Surf. Sci.* **2000**, 459, 213.
- (7) Sun, Q.; Shen, B. R.; Fan, K. N.; Deng, J. F. *Chem. Phys. Lett.* **2000**, 322, 1.
- (8) Van Santen, R. A.; Kuipers, H. P. C. *Adv. Catal.* **1990**, 35, 256.
- (9) Grail, P. A.; White, J. A.; Bird, D. M. *Surf. Sci.* **1996**, 352–354, 248.
- (10) Ricart, J. M.; Torras, J.; Clotet, A.; Sueiras, J. E. *Surf. Sci.* **1994**, 301, 89.
- (11) Salazar, M. R.; Saravanan, C.; Kress, J. D.; Redondo, A. *Surf. Sci.* **2000**, 449, 75.
- (12) Milov, M. A.; Zilberberg, I. L.; Ruzankin, S. Ph.; Zgidomirov, G. M. *J. Mol. Catal. A: Chem.* **2000**, 158, 309.
- (13) Rocca, M.; Savio, L.; Vattuone, L.; Palomba, U.; Novelli, N.; Buatier de Mongeot, F.; Valbusa, U. *Phys. Rev. B* **2000**, 61, 213.
- (14) Vattuone, L.; Rocca, M.; Restelli, P.; Pipo, M.; Boragno, C.; Valbusa, U.; *Phys. Rev. B* **1994**, 49, 5113.
- (15) Ares Fang, C. S. *Surf. Sci.* **1990**, 235, L291.
- (16) Buatier de Mongeot, F.; Rocca, M.; Cupolillo, A.; Valbusa, U. *J. Chem. Phys.* **1997**, 106, 711.
- (17) Buatier de Mongeot, F.; Cupolillo, A.; Rocca, M.; Valbusa, U. *Chem. Phys. Lett.* **1999**, 302, 302.
- (18) Savio, L.; Vattuone, L.; Rocca, M. *Phys. Rev. B* **2000**, 61, 7324.
- (19) Torras, J.; Ricart, J. M.; Illas, F.; Rubio, J. *Surf. Sci.* **1993**, 297, 57.
- (20) Ricart, J. M.; Torras, J.; Illas, F.; Rubio, J. *Surf. Sci.* **1994**, 307, 107.
- (21) Kresse, G.; Hafner, J. *Phys. Rev. B* **1993**, 47, 558.
- (22) Kresse, G.; Furthmüller, J. *Comput. Mater. Sci.* **1996**, 6, 15.
- (23) Kresse, G.; Furthmüller, J. *Phys. Rev. B* **1996**, 54, 11169.
- (24) Vanderbilt, D. *Phys. Rev. B* **1990**, 41, 7892.
- (25) Kresse, G.; Hafner, J. *J. Phys. Condens. Matter* **1994**, 6, 8245.
- (26) Perdew, J. P.; Chevary, J. A.; Vosko, S. H.; Jackson, K. A.; Pederson, M. R.; Singh, D. J.; Fiolhais, C. *Phys. Rev. B* **1992**, 46, 6671.
- (27) Methfessel, M.; Paxton, A. T. *Phys. Rev. B* **1989**, 40, 3616.
- (28) Wang, Y.; Wang, W. N.; Fan, K. N.; Deng, J. F. *Surf. Sci.* **2001**, 490, 125.
- (29) Makov, G.; Payne, M. C. *Phys. Rev. B* **1995**, 43, 4014.
- (30) Neugebauer, J.; Scheffler, M. *Phys. Rev. B* **1992**, 46, 16067.
- (31) Monkhorst, H. J.; Pack, J. D. *Phys. Rev. B* **1976**, 3, 5188.
- (32) Liem, S. Y.; Kresse, G.; Clarke, J. H. R. *Surf. Sci.* **1998**, 415, 194.
- (33) Engelhardt, H. A.; Menzel, D. *Surf. Sci.* **1976**, 57, 591.
- (34) Fan, K. N.; Shen, B. R.; Wang, W. N.; Deng, J. F. *J. Mol. Struct. (THEOCHEM)* **1998**, 422, 191.
- (35) Wang, Y.; Wang, W. N.; Fan, K. N.; Deng, J. F. *Surf. Sci.* **2001**, 487, 77.